

# Activation of TrkA<sup>+</sup> Nerves Induces Calvarial Defect Healing and Mesenchymal TGF- $\beta$ Signaling

Zhao Li<sup>1</sup>, Xin Xing<sup>1</sup>, Austin Z Chen<sup>1</sup>, Mary Archer<sup>1</sup>, Collin Wang<sup>1</sup>, Qizhi Qin<sup>1</sup>, Manyu Zhu<sup>1</sup>, Masnsen Cherief<sup>1</sup>, Mingxin Xu<sup>1</sup>, Thomas L Clemens<sup>2</sup>, Aaron W James<sup>1\*</sup>.

<sup>1</sup>Department of Pathology, Johns Hopkins University, Baltimore, MD 21205, USA

<sup>2</sup> Department of Orthopaedics, University of Maryland School of Medicine, Baltimore, MD 21201, USA

Presenting author: zli172@jh.edu; \*Corresponding author: awjames@jh.edu

**Disclosures:** AWJ is a consultant for Novadip Biosciences and Lifesprout LLC.

**INTRODUCTION:** The regulatory roles of sensory nerves in bone metabolism are increasingly recognized. Previous studies from our group demonstrate the essential role of neurotrophic tyrosine kinase receptor type 1 (TrkA) signaling for stress fracture repair<sup>1</sup> and calvarial defect healing<sup>2</sup>, indicating that bone repair depends on intact peripheral sensory neural signaling. Other groups have also shown TrkA agonism augments the anabolic response to mechanical load<sup>3</sup>, and improves long bone fracture healing in mice<sup>4</sup>. However, the key pathways whereby TrkA<sup>+</sup> sensory nerves enhance bone repair remain undefined. In this study, we utilized single-cell RNA sequencing of calvarial injury sites to elucidate the critical pathways through which activation of TrkA signaling enhances bone regeneration.

**METHODS:** All experiments were conducted with the approval of IACUC at the Johns Hopkins University. Gambogic amide (GA), a non-peptide small molecule that selectively binds to the juxtamembrane domain of TrkA, was used to activate TrkA signaling. Mice received intraperitoneal (IP) injection of either 100  $\mu$ L vehicle control or 1.2 mg/kg GA ( $n = 6$ ). A 1.8-mm-diameter, full-thickness, circular frontal calvarial defect was created. For single-cell RNA-Seq ( $n = 4$ ), skulls were microdissected 7 days after injury, digested with collagenase type I/II, and processed by 10X Genomics. Sequenced single cell reads were aligned to a mouse reference transcriptome (mm10-2020-A) using Cell Ranger 7.1.0. Output files were analyzed using Scanpy, Scvelo, Decoupler, Monocle2, Cellchat, and pySCENIC. Analysis of cell-cell communication was performed by integrating single-cell RNA sequencing datasets of trigeminal ganglia neurons with calvarial injury sites<sup>5</sup>. MicroCT and histology on skulls was performed 28d post-operative. Histology and immunofluorescent staining (GAP-43 and OCN) was performed.

**RESULTS:** Gambogic amide (GA) treatment enhanced bone healing compared to controls, with quantitative micro-CT showing increased bone volume (65.9%, **Fig. 1A**), increased axon growth into the bone injury site (223%, **Fig. 1B**), and increased osteocalcin expression (97.6%, **Fig. 1C**). Using scRNA-seq data, unsupervised clustering identified five mesenchymal cell subclusters within the calvarial injury site (**Fig. 1D**), which were annotated as cell types using known marker gene expression, including stem cell markers (*Cd34*, *Thy1*), proliferation markers (*Ube2c*, *Mki67*), multilineage progenitor markers (*Scx*, *Clec11a*), osteoblast markers (*Spp1*, *Bglap*), and fibroblast markers (*Col4a1*, *Eln*) (**Fig. 1E**). Trajectory analysis revealed differentiation trajectories towards both osteoblast and fibroblastic cell fates (**Fig. 1F**). Comparison between GA and control groups showed 158% more osteoblasts, but 66% fewer fibroblastic progenitors in the GA group compared to controls (**Fig. 1G**). RNA velocity analysis further supported more osteoblast differentiation with GA treatment (**Fig. 1H**). Module score analysis using MSigDB hallmark gene sets revealed differential pathway activity (**Fig. 1I**), with pseudotime analysis showing increased TGF- $\beta$  signaling pathway activity especially in middle and late pseudotime. Expression of TGF- $\beta$  pathway-related genes was significantly higher in the GA group compared to the Ctrl group, including increased expression of *Fmod*, *Tgfb2* and *Bmpr2* (**Fig. 1J**). Interactome comparison between GA and Ctrl groups showed stronger predicted TGF- $\beta$  pathway interactions with GA treatment, primarily the ligand *Tgfb2* originating from non-peptidergic (NP) TrkA<sup>+</sup> neurons (**Fig. 1K**). Together, this demonstrates the activation of TrkA<sup>+</sup> nerves enhances calvarial defect healing likely through stimulating TGF- $\beta$  signaling pathways.

**DISCUSSION:** In this study, we activated TrkA signaling using gambogic amide (GA) and demonstrated greater nerve ingrowth into the injured bone and enhanced bone repair. Our single-cell RNA sequencing analysis revealed that increased neural ingrowth is associated with stimulation of the TGF- $\beta$  signaling pathway. Our previous work shows TrkA agonism increases traumatic heterotopic ossification, and TrkA activation shifts local TGF $\beta$  signaling<sup>6</sup>, suggesting neural-derived TGF $\beta$  regulates bone formation. Collectively, these findings indicate TGF $\beta$  signaling is involved in neurogenically stimulated bone formation. GA facilitates NGF-TrkA signaling activity through allosteric activation. While NGF causes transient TrkA activation and degradation, GA induces lower but more sustained TrkA phosphorylation. Given its affordability, tolerability, and availability, the small molecule GA represents a promising pharmacological approach for bone regeneration. Delineating the mechanisms whereby neurogenic activation enhances bone repair will enable optimization of pro-regenerative strategies for translation to the clinic.

**SIGNIFICANCE/CLINICAL RELEVANCE:** Understanding the signaling pathways underlying neurogenically-enhanced bone repair will facilitate development of novel pharmacological strategies to improve clinical outcomes. Targeted activation of the TrkA pathway represents a promising approach to accelerate healing after bone injury.

**REFERENCES:** 1. Z. Li *et al.*, doi: 10.1172/JCI128428. 2. C. A. Meyers *et al.*, doi: 10.1016/j.celrep.2020.107696. 3. G. Fioravanti *et al.*, doi: 10.1016/j.bone.2021.115908. 4. M. R. Johnstone *et al.*, PMID: 30839307. 5. L. Yang *et al.*, doi: 10.1016/j.neuron.2022.03.003. 6. M. Cherief *et al.*, doi: 10.1093/stcltm/szac073.

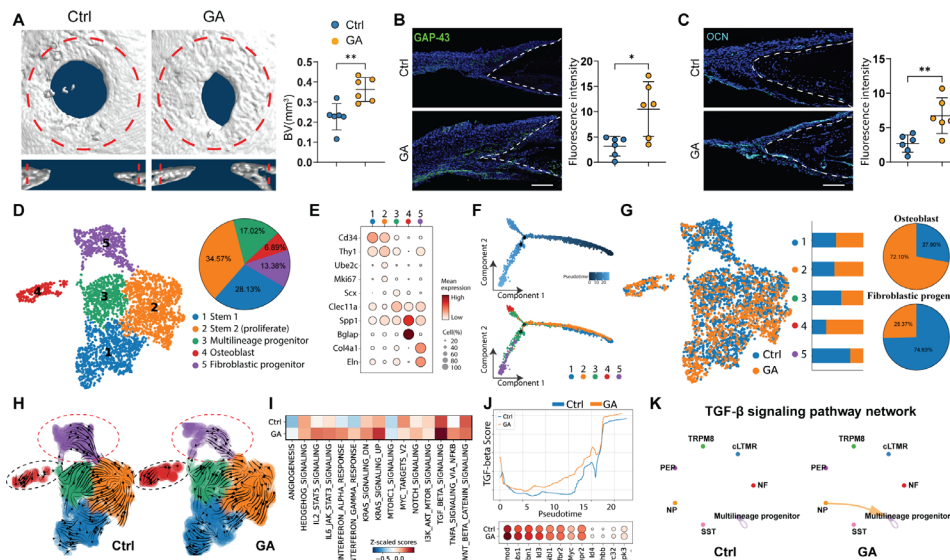


**Figure 1. TrkA agonism using gambogic amide improves calvarial bone defect repair and scRNAseq analysis** (A) Micro-CT reconstructions of the defect site in a top-down view (above) and coronal cross-sectional images (below) at 28 days post-injury. Margins of original defect are indicated by red dashed lines. Micro-CT quantification of bone healing among GA- and vehicle-injected mice, including bone volume (BV), (B) (C) Immunohistochemical staining of GAP43 and OCN at the defect edge and quantification of immunoreactivity within the calvarial defect site at 28 days post-injury. (D) UMAP plots and percent of each cluster. (E) Dot plot of marker gene expression (F) Trajectory of mesenchymal cells to osteoblasts inferred by Monocle2 and colored by cell clusters. (G) Distribution in UMAP plot and percent of osteoblast and fibroblastic progenitor from GA and Ctrl mice. (H) RNA velocity analysis: red dashed circle (fibrogenesis), black dashed circle (osteogenesis) (I) Matrix plot of pathway signaling activity. (J) Changes in pathway activity scoring across pseudotime and dot plot showing expression of pathway-related genes. (K) Hierarchy plot compared TGF- $\beta$  signaling pathway between Ctrl and GA. Each dot represents a single animal.  $n = 6$  animals per group.  $p^* < 0.05$  and  $p^{**} < 0.01$  in comparison with vehicle control as assessed using a two-tailed Student's t-test. Data are represented as mean  $\pm$  SD. Scale bars, 100  $\mu$ m.